Common Mode Filter for EMI Mitigation in Active Phase Converter

Anil K Adapa, Vinod John
Department of Electrical Engineering
Indian Institute of Science, Bangalore, Karnataka, India
Email: anila@iisc.ac.in, vjohn@iisc.ac.in

***Abstract*—This paper proposes a common-mode (CM) filter based on a reduced switch active phase converter (APC) topology. The CM filter configuration provides a parallel path for CM currents in the unsymmetrical three-phase converter and reduces the EMI injected into the grid. The proposed CM filter facilitates the independent design of the differential-mode filter components of the converter. Analysis of the converter system is carried out using state-space approach. From the eigenvalue analysis of the system, it is shown that inclusion of the proposed CM filter does not affect the existing APC system poles. Hence, no filter redesign of the control structure is required. A design methodology is approved to select the CM filter components that can actively damp the CM resonance without any additional control loop. Efficacy of the proposed filter configuration is validated experimentally by measuring the common-mode voltage with the laboratory APC feeding a three-phase 3 hp induction motor from a single-phase grid.**

***Index Terms*—Active phase converter, Common mode noise, Voltage source inverter, Common mode filter, Closed loop control.**

I. Introduction

Insulated Gate Bipolar Transistor (IGBT) based power electronic converters are widely used in most of the power conversion and conditioning applications over a wide power range. Switching action of the power semiconductor devices in the power converter produces undesirable common mode voltage (CMV), which excites the parasitic capacitors that occur in the physical structures of the converter ground. Fig. 1(a) shows a typical drive system that includes parasitic capacitors at different locations, namely the machine rotor to the frame, stator to the frame, rotor to stator and cables to ground. Also, parasitic capacitors occur between the incoming power supply cables to the ground, and power converter cabinet, often between the power semiconductor devices and heat-sink. The converter cabinets and frame need to be grounded for safety reasons. These parasitic capacitors provide a path to common mode current (CMC) and cause EMI/EMC problems and observable ground leakage currents [1]–[5].

The continual development of the power semiconductor devices to improve efficiency and power density

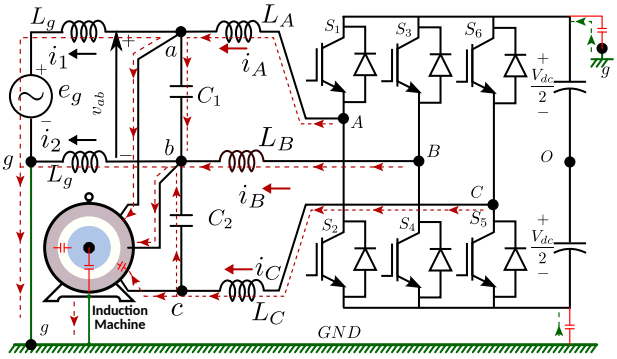

Fig. 1: Active phase converter (APC) system indicating parasitic capacitors at different locations and common-mode current (CM) paths.

[6] has given a great impetus to the newer generation devices with increased switching speed and reduced power loss. The effect of CMV is more pronounced with semiconductor devices having sharp turn-on and turn-off characteristics. This produces higher dv/dt voltages with steep-fronted CMV. Increased switching frequency and dc link voltage accentuate EMI/EMC issues. This common mode voltage and current have detrimental effects like premature bearing failures in drives [1], and interference with the control and communication circuitry of the converter [3].

For a dc link voltage, V_{dc} of a three-phase power converter, CMV may take any value of $\pm V_{dc}/2$ or $\pm V_{dc}/6$, depending on the converter switching state. Conventional sine triangular pulse width modulation and space vector modulation (SVM) techniques produce peak CMV as high as half the dc link voltage and CMV changes by $\pm V_{dc}/3$ every time the switching state changes [3]. To reduce the CMV, a number of reduced common mode voltage PWM techniques that uses non zero vectors to synthesize zero vectors are proposed in literature [2], [3], [5]. All these PWM techniques have implications on the operable range of modulation index and introduce simultaneous switching of the power converter [3].

Passive CM filters are available that bypass the CM noise from ac side to the dc link with an alternate low impedance path [7]–[10]. CM chokes mitigate the

978-1-5386-1180-7/18/$31.00 ©2018 IEEE

CM current (CMC) that injects into the grid or bearing current of the motor drive. However, CM chokes in these designs are bulky as they carry load current. Effect of CMV can be reduced by employing dv/dt filter which tailors the steep-fronted converter pole voltage [11]. The dv/dt filters use smaller filter components and have a resonant frequency higher than the switching frequency. This calls for passive damping which makes the filter less efficient at higher frequencies due to significant power loss [11], [12].

Various active common mode filter topologies are proposed to mitigate the CMV [13], [14], which require additional power converter or semiconductor switches. The active CM filter for grid-connected PV systems without isolation presented in [13] consists of a CM transformer and a low power full bridge connected to the third winding. The low power converter compensates the CM voltage by transformer action. The CM transformers, besides the difficulty in adding to the established converter, they are bulky in size, not easy to design and manufacture [14]. A hybrid filter proposed in [14] uses a carrier peak position modulation (CPPM) to ensure only two level CMV at the inverter output and a half bridge active CM filter connected to the neutral point of the DM filter. In spite of the simple approach proposed for a three-phase three wire system, the method has a limitation in deriving the dc link for the active CM filter and is limited to the CPPM technique.

The CM filter topologies and the design procedure given are typically for symmetrical three-phase or single-phase systems. Also, customized CM filter solutions that are best suited for a specific converter topology are present in literature [13]–[15]. Reduced switch single-phase to three-phase converters are an attractive solution in remote areas and rural communities where only single-phase supply is available [16]. Fig. 2 shows active phase converter based on the reduced switch single-phase to three-phase converter presented in [16], [17].

This paper describes a passive CM filter configuration for reduced switch active phase converter. Effect of the CM filter is analyzed by eigenvalue analysis of the state matrix obtained for the active phase converter with the proposed CM filter configuration. The CM filter design procedure outlines a method for a prudent choice of the different CM filter components. Also, the proposed CM filter configuration and the selection method does not require a redesign of the hardware and control of the active phase converter topology considered.

II. CM Filter Configuration

A. Active Phase Converter

The active phase converter connected to the grid with an LCL filter and maintains the dc link at the desired voltage level. Grid voltage at the point of common coupling v_{ab} serves as a line to line voltage for a three-phase load. Controlling the converter generated line voltage v_{cb}, the active phase converter provides balanced three-phase voltage to the load. The converter legs A and B act as a front end converter and legs B and C act as an inverter, leg-B being the shared leg between FEC and inverter. Design of LCL filter of the grid-connected FEC and LC filter of the inverter and control loops can be carried out independently [16]. Decoupled control methods of the converters with a shared leg are presented in [16], [18].

CM filter design of LCL filter based grid-connected converters and LC filter based inverters for motor drives are well established in literature [4], [9], [12]. These methods incorporate the single-phase equivalent circuit to analyze the CMC paths and design the appropriate filter components that are sufficient for the considered application.

B. Proposed CM Filter Configuration

Proposed CM filter configuration for the active phase converter is shown in Fig. 2. The CM filter capacitor C_{CM}, in Fig. 2(a) is connected between the node b at the point of common coupling and the dc link midpoint, O. For the converter configurations with inaccessible dc link midpoint, split CM capacitors are used and the common point of those capacitors M is connected to the node b as shown in Fig. 2(b). The CM filter capacitor provides a path to circulate the CM currents within the converter, thus mitigating the CM currents injecting into the grid. The high-frequency ringing noise at node b (same as M) due to the PWM switching can be brought down to ground potential by earthing. But, this results in ground current injection which is limited only by the grid side impedance [12]. This can be reduced by a suitable capacitor C_{Mg} connected between the node b and the ground, g. High-frequency resonance caused by the inclusion of C_{Mg}, which is typically few tens of pF, need to be damped by passive means.

1) Functional Description of CM Filter: The functionality of the proposed CM filter configuration in the current section and analysis given in the section-III is based on simplifying assumption of no C_{Mg} connected and the converter is under no load. Typical load impedance will be higher than the filter inductance and inductive in nature, hence CMC, i_{CM} flow through the capacitively coupled low impedance path provided by the CM filter as shown in the Fig. 2(a) and (b).

The CM filter capacitor C_{CM} connected between node b and dc link midpoint O plays a role in preventing CMV at the dc-link and provides low impedance path to circulate switching frequency CMC within the converter. The differential mode filter capacitors C_1 and C_2 of the FEC and inverter provide a low impedance path for CMC

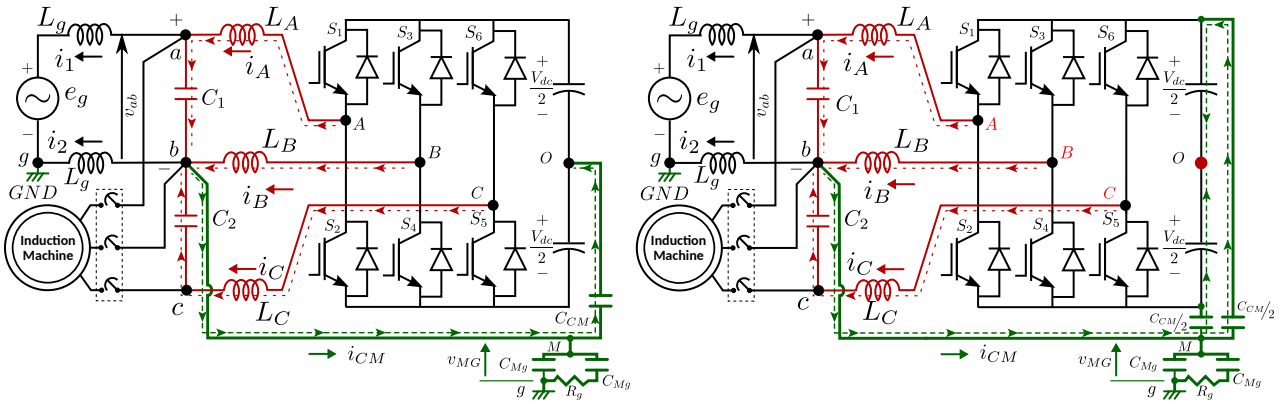

(a) (b)

Fig. 2: Common mode filter configuration for the active phase converter indicating the prevalent paths to the CMC. (a) case when dc-bus midpoint available (b) case when dc-bus midpoint is unavailable.

from the converter poles A and C to the node b. The CMC paths are indicated in Fig. 2(a). In the absence of the CM filter capacitor C_{CM}, total CMC will be injected into the ground through grid and machine winding to frame capacitance. With the CM filter capacitor C_{CM}, CMC can be averted from being injected into the grid and returns to the dc link midpoint through C_{CM} and hence $i_{CM} \approx i_A + i_B + i_C$.

The floating node O or M can attain any potential with respect to the ground, depending on the parasitic coupling, and this voltage can be brought as close as possible to the ground potential by connecting C_{Mg}.

The order reduction achieved in the common-mode equivalent circuit during its derivation is due to the symmetry of the power circuit path. The reduced switch active phase converter shown in Fig. 2 has the combination of LCL filter based grid-connected front end converter and an LC filter based inverter. This makes the converter configuration an unique, asymmetrical three-phase system. Hence, invoking a single phase equivalent circuit approach to simplify the analysis is not feasible. Hence, a full circuit analysis is used to obtain the dynamical equations of the APC power circuit.

C. Eigenvalue Analysis

The active phase converter shown in the Fig. 2 has five filter inductors, two differential filter capacitors and one CM filter capacitor. Current through inductors and capacitor voltages are taken as the state variables to obtain dynamic equations of the system as given below.

$$L_A \frac{d}{dt} i_A = -v_{ab} - v_{bO} + v_{AO} \tag{1}$$

$$L_B \frac{d}{dt} i_B = -v_{bO} + v_{BO} \tag{2}$$

$$L_C \frac{d}{dt} i_C = -v_{cb} - v_{bO} + v_{CO} \tag{3}$$

$$L_g \frac{d}{dt} i_1 = v_{ab} + v_{bO} + v_{AO} + v_{Og} \tag{4}$$

$$L_g \frac{d}{dt} i_2 = v_{bO} + v_{Og} \tag{5}$$

$$C_1 \frac{d}{dt} v_{ab} = i_A - i_1 \tag{6}$$

$$C_2 \frac{d}{dt} v_{cb} = i_C \tag{7}$$

$$C_{CM} \frac{d}{dt} v_{bO} = i_A + i_B + i_C - i_1 - i_2 \tag{8}$$

where, v_{Ag}, v_{Bg} and v_{Cg} converter pole ground voltages. e_g is the grid supply voltage and v_{Og} represents converter mid-point to ground voltage that is excited by external circuits, that are not explicitly indicated in the Fig. 2(a) and (b). System dynamics characterized by (1) through (8), can be represented with a state matrix, $\mathbf{x}$ of eight state variables, as below

$$\dot{\mathbf{x}} = \mathbf{A}\mathbf{x} + \mathbf{B}\mathbf{u} \tag{9}$$

where,

$$\mathbf{A} = \begin{bmatrix} 0 & 0 & 0 & 0 & 0 & \frac{-1}{L_A} & 0 & \frac{-1}{L_A} \\ 0 & 0 & 0 & 0 & 0 & 0 & 0 & \frac{-1}{L_B} \\ 0 & 0 & 0 & 0 & 0 & 0 & \frac{-1}{L_c} & \frac{-1}{L_c} \\ 0 & 0 & 0 & 0 & 0 & \frac{1}{L_g} & 0 & \frac{1}{L_g} \\ 0 & 0 & 0 & 0 & 0 & 0 & 0 & \frac{1}{L_g} \\ \frac{1}{C_1} & 0 & 0 & \frac{-1}{C_1} & 0 & 0 & 0 & 0 \\ 0 & 0 & \frac{1}{C_2} & 0 & 0 & 0 & 0 & 0 \\ \frac{1}{C_{CM}} & \frac{1}{C_{CM}} & \frac{1}{C_{CM}} & \frac{-1}{C_{CM}} & \frac{-1}{C_{CM}} & 0 & 0 & 0 \end{bmatrix}$$

$$\mathbf{x} = [i_A \quad i_B \quad i_C \quad i_1 \quad i_2 \quad v_{ab} \quad v_{cb} \quad v_{bO}]^T$$

$$\mathbf{u} = [v_{Ag} \quad v_{Bg} \quad v_{Cg} \quad e_g \quad v_{Og}]^T$$

Roots of the system characteristic equation (CE) correspond to circuit, the eigen values can be obtained from the A matrix using (10).

$$|s\mathbf{I} - \mathbf{A}| = 0 \tag{10}$$

The active phase converter differential filter components tabulated in Table. I. Eigenvalues of the **A** matrix are found with three different values of the C_{CM} that are used in the APC are given in the Table. II

TABLE I: Active phase converter circuit parameters.

Hardware Details	
FEC Filter inductance, L_A and L_B	1.5 mH
FEC Filter Capacitance, C_1	4.0 μF
Inverter Filter inductance, L_C	1.5 mH
Inverter Filter Capacitance, C_2	2.0 μF
Grid side inductance, L_g	1.0 mH
DC link Voltage, V_{dc}	800 V
Switching frequency, $f_{sw}(=\frac{1}{T_{sw}})$	25 kHz
Sampling frequency, $f_s(=2f_{sw})$	50 kHz
CM filter capacitance, C_{CM}	2×0.47 μF
CM filter to ground capacitance, C_{Mg}	15 nF ‖ (15 nF+68 Ω)

TABLE II: Variation of eigen values of the system with common mode filter capacitance, C_{CM}

C_{CM}	frequency of resonant pole pair			
	$\pm\lambda_{1,2}$	$\pm\lambda_{3,4}$	$\pm\lambda_{5,6}$	$\pm\lambda_{7,8}$
2 nF	275.67 kHz	3.9 kHz	2.7 kHz	0 kHz
0.2 μF	27.62 kHz	3.9 kHz	2.7 kHz	0 kHz
2 μF	8.9 kHz	3.86 kHz	2.67 kHz	0 kHz

Roots of the CE, or eigenvalues of the **A** matrix, can be obtained by solving (10). The resonant frequencies f_1, f_2, f_3 and f_4 correspond to 4 pairs of complex eigenvalues of the CE. One of the resonant frequencies, f_4 corresponds to the eigenvalues, λ_7 and λ_8 at the origin. Table-II shows the variation of resonant frequencies with a change in C_{CM}. Though the variation of common mode filter capacitor, C_{CM} is significant, the consequential effect of the C_{CM} on the resonant frequencies f_2 and f_3 is imperceptible, whereas f_1 corresponding to the two eigenvalues λ_1 and λ_2 that exhibits remarkable shift with change of C_{CM}.

D. Effect of C_{CM} on converter control

From the eigenvalue analysis, it is evident that the C_{CM} does not significantly affect the remaining APC power circuit poles. Hence, designed current control of

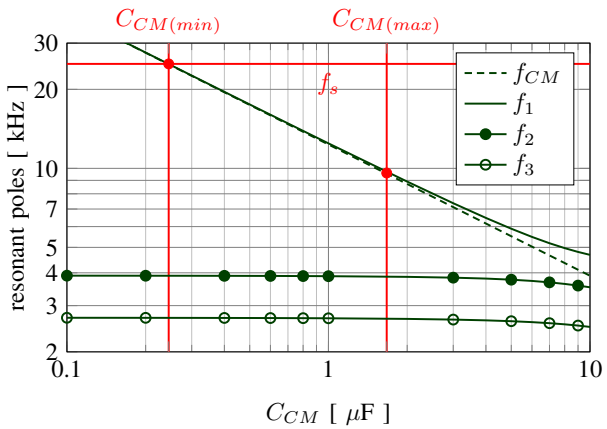

Fig. 3: Variation of resonant poles with change of C_{CM}

FEC and Inverter, considering only the differential mode filters will be effective for the intended operation of the active phase converter, even after connecting the C_{CM}. For the selected CM filter C_{CM} parameter of 0.94 μF, from eigenvalue analysis, CM resonant frequency, f_1, is found to be 12.8 kHz which is lower than the Nyquist frequency, f_{sw}. The value of C_{CM} for the circuit is selected so that the eigenvalue affected by C_{CM} has an eigenfrequency sufficiently below f_{sw}. Hence the existing current control loops can provide sufficient damping to the resonance detected by the sensed CM currents. This approach to C_{CM} selection allows one to use the existing current control loop, which can provide damping to filter resonances [12]. A selection criterion for the C_{CM} based on the minimum and maximum allowable limits on C_{CM} for the APC is explained in the Section-IV.

Key points of the eigen value analysis can be summarized as follows:

- Order of the system : 8
- Number of roots : 4 complex pole pairs
- Effect of C_{CM} : Predominantly on one pole pair and marginal on other poles
- The common mode filter capacitor C_{CM} does not effect the existing differential mode converter control

III. Common Mode Equivalent Circuit

A. Proposed CM Equivalent Circuit

In this section, an approximate behavioral equivalent circuit for APC with the proposed CM filter is developed. In a symmetrical three-phase FEC with LCL-filter or a three-phase inverter with LC-filter, a simplified CM equivalent circuit is derivable. The simplified circuit reduces the order of the system, thus facilitating to design the CM-filter components. In an asymmetrical converter like APC, the CM currents have different paths

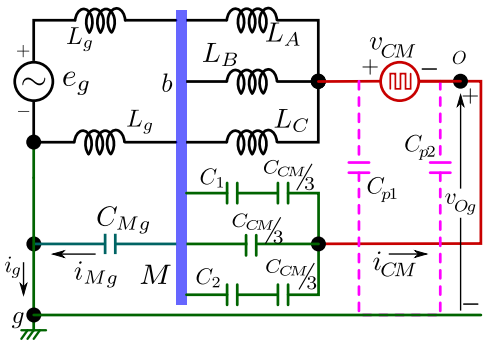

Fig. 4: Proposed behavioral CM equivalent circuit of the APC including the CM filter.

with distinct impedance in each path. Thus, representing the APC system with the CM-filter by an analytically derivable CM equivalent circuit is not feasible. Based on the prevailing paths for the CMC as indicated in the Fig. 2 an approximate behavioral CM equivalent circuit is proposed.

A CM equivalent circuit, that captures the behavior of the dominant pole pair introduced in the system, due to the C_{CM} as explained in the eigenvalue analysis. The proposed CM equivalent circuit is useful in dimensioning the CM filter capacitance C_{CM} for a given APC with pre-designed differential mode filters. For the following analysis, the capacitance C_{Mg} is not considered, which is typically very small and serves in bypassing the leakage currents due to the parasitic capacitances of the APC system. The capacitor C_{p1} in the Fig. 4 represents the semiconductor device collector to ground and dc-bus to ground parasitic capacitances in the APC system. The capacitor C_{p2} in the Fig. 4 represents the converter poles and cables to ground parasitic capacitances.

The common-mode current (CMC) component through three legs of the converter, in Fig. 2 are considered to be $i_{CM(A)}$, $i_{CM(B)}$ and $i_{CM(C)}$, follows the relation given by (11).

$$i_{CM} = i_{CM(A)} + i_{CM(B)} + i_{CM(C)} \tag{11}$$

The common mode current (CMC), given in (11), referring to the Fig. 2 has the following paths,

(i) Path-1: $i_{CM(A)} \Rightarrow L_A \rightarrow C_1 \rightarrow C_{CM}$.

(ii) Path-2: $i_{CM(B)} \Rightarrow L_B \rightarrow C_{CM}$.

(iii) Path-3: $i_{CM(C)} \Rightarrow L_C \rightarrow C_2 \rightarrow C_{CM}$.

The approximate CM equivalent circuit is developed by forming a super node b (or M) to which the CM source, v_{CM} is connected with a lumped inductance and capacitance with multiple parallel branches as shown in the Fig. 4.

The resultant approximate equivalent circuit has one lumped series inductance L_{con} and one lumped series capacitance C_{eq} given in (12).

$$\begin{aligned} L_{con} &= L_A \parallel L_B \parallel L_C, \\ L_{eq} &= L_{con} \parallel \frac{L_g}{2} \quad \text{and} \\ C_{eq} &= \left(C_1 + \frac{C_{CM}}{3}\right) \parallel \frac{C_{CM}}{3} \parallel \left(C_2 + \frac{C_{CM}}{3}\right) \end{aligned} \tag{12}$$

The transfer function of $\frac{i_{g(s)}}{v_{Og}}$ is given in (13),

$$\frac{i_{g(s)}}{v_{Og}} = \frac{s^2 L_{con} C_{eq}}{s(\frac{L_g}{2} + L_{con})(s^2 L_{eq} C_{eq} + 1)} \tag{13}$$

The resonant pole of (13) due to the C_{CM} is given in (14)

$$f_{CM} = \frac{1}{2\pi\sqrt{L_{eq} C_{eq}}} \tag{14}$$

where,

$$\begin{aligned} L_{eq} &= \left(\frac{1}{L_A} + \frac{1}{L_B} + \frac{1}{L_C} + \frac{2}{L_g}\right)^{-1} \\ C_{eq} &= (1 + \alpha + \beta)\frac{C_{CM}}{3} \\ \alpha &= \frac{3C_1}{3C_1 + C_{CM}} \quad \text{and} \quad \beta = \frac{3C_2}{3C_2 + C_{CM}} \end{aligned} \tag{15}$$

It is observed that the resonant frequency, f_{CM} given by empirical formula given in (14) is in close agreement with the resonant frequency, f_1 obtained from the eigenvalue analysis, especially for the values of C_{CM} that are less than the DM filter capacitances.

Fig. 3 shows the resonant frequencies due to complex pole pairs of the eigenvalues. The resonant frequency f_1 obtained from the eigenvalue analysis is in close agreement with the resonant frequency given by (14). This validates that the proposed approximate equivalent circuit is given in the Fig. 4 can be used for further analysis to design the CM filter components of the APC of Fig. 2.

IV. CM Filter Design

Selection procedure for the CM filter components C_{CM}, C_{Mg} and R_g is outlined in this section.

The parasitic capacitances C_{p1} and C_{p2} is in the order of few tens of picofarad [15], [19]. The capacitor C_{Mg} should be more than the effective parasitic capacitance as discussed in the section-IV(B). Its typical value is less than C_{CM} and it offers high impedance near the switching frequency. Hence, C_{Mg} is ignored in the low-frequency approximation of the equivalent CM circuit shown in the Fig. 5(b). For higher frequencies beyond few hundreds of kHz, the differential mode inductances offer very high impedance and hence they are replaced with an open circuit and C_{CM} with a short circuit. The

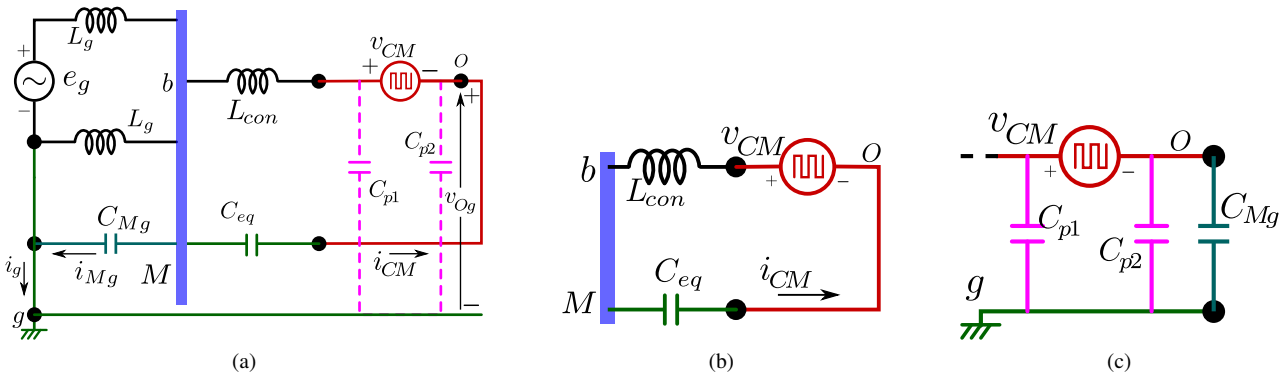

Fig. 5: Behavioral CM equivalent circuit of the APC. (a) Simplification of proposed CM equivalent circuit. (b) Low frequency approximation. (c) High frequency approximation.

high-frequency approximation of the equivalent circuit is given in the Fig. 5(c).

A. Selection of C_{CM}

From the low frequency approximation of the CM circuit given in the Fig. 5(b), the transfer function of $\frac{I_{CM}}{V_{CM}}$ is given in (16).

$$\frac{I_{CM}}{V_{CM}} = \frac{sC_{eq}}{s^2 L_{con} C_{eq} + 1} \tag{16}$$

Addition of the C_{CM} to the original APC differential filter circuit increases the order of the system by bringing one more resonant pole. The additional resonance due to C_{CM} can be damped by active or passive means. No power loss involved in active damping makes it an attractive choice over the passive damping. For effective damping of the CM resonant frequency, the pole location or f_1 should be within the available bandwidth of the APC inner current control loop. Hence, the switching frequency and the sampling method adopted gives the lower limit of C_{CM} below which active damping is not possible. Passive damping can relax the limit further. For lower values of the C_{CM}, $\alpha \approx 1$ and $\beta \approx 1$. This gives the following condition for the minimum value for $C_{CM(min)}$, as seen in (15),

$$\begin{aligned} \frac{1}{2\pi\sqrt{L_{con}C_{eq}}} &\leq \frac{f_s}{2} \\ \Rightarrow \frac{1}{2\pi\sqrt{L_{con}C_{CM(min)}}} &\leq \frac{f_s}{2} \end{aligned} \tag{17}$$

where, f_s is the sampling frequency of the digital controller.

Hardware details of the APC are given in the Table-I. The sampling frequency f_s used in the experimental validation is 50 kHz. The $C_{CM(min)}$ obtained for the APC using the relation given in (17) is 0.25 μF.

The maximum value of CM filter capacitor $C_{CM(max)}$ is obtained by fixing the limit on fundamental current carried by the C_{CM}. Here the limit is chosen to be 2.5% of the fundamental. The fundamental current carried by the C_{CM} is limited by the maximum fundamental pole voltage v_{BO}. The load in the laboratory APC setup is a 3hp/415V induction machine drawing a line current of 4.6 A. The $C_{CM(max)}$ is 1.6 μF which corresponds to the laboratory APC prototype and the load current. The chosen C_{CM} is 0.94 μF.

B. Selection of C_{Mg}

Typical value for C_{Mg} is very small compared to C_{CM}. The resonance caused by C_{Mg} has to be damped passively. To simplify the eigen value analysis, C_{Mg} is not included in the state space representation of the system in (9). The high-frequency equivalent circuit for a symmetrical three-phase system is given in [12], [19]. A similar approach is used to obtain the same for the active phase converter shown in Fig. 2(a) and (b). In order to minimize the voltage v_{Mg}, the value C_{Mg} should be high compared to the parasitic capacitances, C_{p1} and C_{p2}. Higher values for C_{Mg} capacitance increases the ground leakage currents and can affect the earth fault detection relays if employed in the system. Hence, selection of C_{Mg} is a trade-off between attenuation of the CM voltage and the earth leakage current. In this case, 95% attenuation to CM given by (18) is taken into consideration for the design.

$$\frac{V_{Mg}}{V_{CM}} \approx \frac{V_{Og}}{V_{CM}} = \frac{C_{p1}}{C_{p1} + C_{p2} + C_{Mg}} \tag{18}$$

The semiconductor device junction to the case can be found from the device data-sheet, and case to heat sink capacitance need to be estimated from the properties of thermal interface material. These capacitances are used to obtain the parasitic capacitance C_{p1} and C_{p2}. The effective parasitic capacitance, C_{p2} is estimated by considering a parallel plate capacitor between the discrete IGBT and the heat sink used in the experimental prototype. The area of each plate is same as that of the

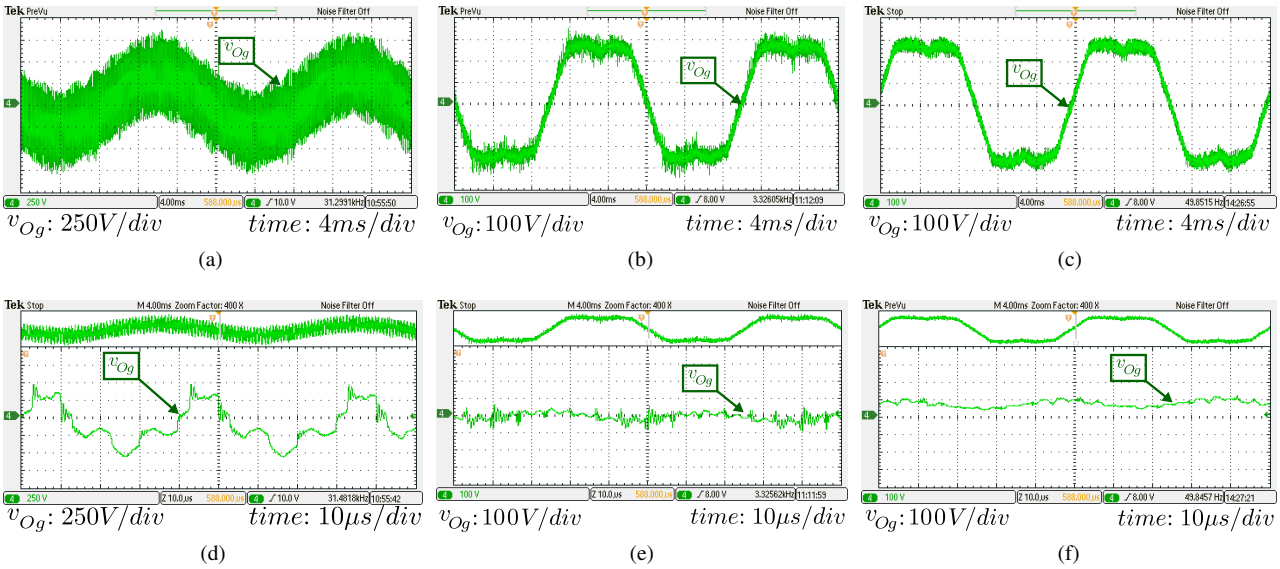

Fig. 6: Common mode voltage (dc bus mid-point to ground voltage) and common mode current for different cases of the CM filter; (a) and (d) no CM filter; (b) and (e) only $C_{CM}/2$ capacitors; (c) and (f) both $C_{CM}/2$ and C_{Mg}.

TO247 device tab and distance between them is equals to the thickness of the thermal interface material whose dielectric constant is found from the data-sheet. The estimated parasitic capacitance is 11 pF. In the experimental prototype, the parasitic capacitance is measured by an LCR meter at 150 kHz and found to be close to 14 pF, Hence, a 15 nF capacitance is used for C_{Mg}.

C. Selection of R_g

The resonant frequency due to C_{Mg} is very high and often beyond f_{sw}. Hence, the resonance introduced by C_{Mg} is damped by passive means. A series connected branch of C_{Mg} and R_g is added parallel to the C_{Mg} as shown in the Fig. 2. Without the additional branch to damp the oscillations, the resonant frequency is measured experimentally, from which the inductance of the ground loop L_p is estimated. The measured resonant frequency is 270 kHz and L_p is 24 μH. For a split capacitor the optimum resistance, R_g that gives maximum damping factor [20] is given by (20). For the experimental prototype the selected R_g is 68 Ω.

$$R_{g(min)}=\sqrt{\frac{2L_p}{C_{Mg}}} \quad \text{and} \quad R_{g(max)}=\sqrt{\frac{4L_p}{C_{Mg}}} \tag{19}$$

$$R_g = \sqrt{R_{g(min)}R_{g(max)}} \tag{20}$$

V. Experimental Results

To assess the effectiveness of the proposed common mode (CM) filter, tests under three different conditions are evaluated in the experimental prototype.

1. No common mode filter is added.
2. Only C_{CM} is added and No C_{Mg}.
3. Both C_{CM} and C_{Mg} are present.

Experimental results corresponding to these three cases are shown in Fig. 6. The dc-bus voltage of the APC is 800 V and the grid voltage is 415 V. A 3 hp induction motor under no load is connected to the active phase converter. The CM filter configuration shown in the Fig. 2(b) with two 0.47 μF CM filter capacitors are used for experimental validation. The effective CM filter capacitance C_{CM} is 0.94 μF. The switching frequency peak to peak CMV of 1000 V in Fig. 6(a) and (d) correspond to the case in which no common mode filter is added. The presence of high frequency, f_{sw} and low-frequency fundamental voltage of v_{CM} can be observed. The zoomed in waveforms over two switching periods indicate the stepped waveforms as illustrated in the Fig. 6(d). In the Fig. 6(b) and (e) the CMV is significantly mitigated by adding the split CM filter capacitors $C_{CM}/2$. The peak to peak high-frequency noise in v_{CM} is reduced from 800 V in case(1) to 180 V in case(2). This corresponds to the case in which only C_{CM} is added. Addition of C_{Mg} along with the CM capacitor C_{CM} reduces the high-frequency CMV further, as shown in Fig. 6(c) and (f). It can be seen that the high-frequency component in v_{CM} voltage is now significantly brought down with 45 V peak to peak in the high-frequency component of the waveform. It can be observed that the high-frequency common mode voltage of v_{Og} is significantly reduced by the proposed common mode filter.

VI. Conclusions

An approach to design common-mode (CM) filter for an asymmetrical three-phase converter. The design procedure outlined in this paper is for a three-leg active phase converter, where FEC and inverter have distinct control loops and differential mode ripple filter components which are independently selected. The eigenvalue analysis substantiates that, the inclusion of the CM filter in the proposed method does not disturb existing control structure of the active phase converter by suitable selection of C_{CM}. Also, this approach does not demand additional control loop for active damping of the resonance due to the added CM filter. The method for selection of midpoint to ground capacitance C_{Mg} is also outlined. Experimental measurements on a laboratory APC confirms the high performance that can be obtained using the proposed common mode filter.

References

[1] D. Busse, J. Erdman, R. J. Kerkman, D. Schlegel, and G. Skibinski, "Bearing currents and their relationship to PWM drives," *IEEE Trans. on Power Electron.*, vol. 12, no. 2, pp. 243–252, Mar 1997.

[2] X. Wu, G. Tan, Z. Ye, Y. Liu, and S. Xu, "Optimized common-mode voltage reduction PWM for three-phase voltage-source inverters," *IEEE Transactions on Power Electronics*, vol. 31, no. 4, pp. 2959–2969, April 2016.

[3] A. M. Hava and E. Ün, "Performance analysis of reduced common-mode voltage PWM methods and comparison with standard PWM methods for three-phase voltage-source inverters," *IEEE Transactions on Power Electronics*, vol. 24, no. 1, pp. 241–252, Jan 2009.

[4] M. H. Hedayati, A. B. Acharya, and V. John, "Common-mode filter design for PWM rectifier-based motor drives," *IEEE Trans. Power Electron.*, vol. 28, pp. 5364–5371, Nov 2013.

[5] K. Tian, J. Wang, B. Wu, Z. Cheng, and N. R. Zargari, "A virtual space vector modulation technique for the reduction of common-mode voltages in both magnitude and third-order component," *IEEE Transactions on Power Electronics*, vol. 31, no. 1, pp. 839–848, Jan 2016.

[6] V. D, A. K. Adapa, K. Upamanyu, and V. John, "Low current switching behavior of igbt and associated spurious tripping in inverters employing vce de-saturation protection," in *2016 IEEE International Conference on Power Electronics, Drives and Energy Systems (PEDES)*, Dec 2016, pp. 1–6.

[7] D. Dong, F. Luo, D. Boroyevich, and P. Mattavelli, "Leakage current reduction in a single-phase bidirectional AC-DC full-bridge inverter," *IEEE Transactions on Power Electronics*, vol. 27, no. 10, pp. 4281–4291, Oct 2012.

[8] M. H. Hedayati and V. John, "Novel integrated cm inductor for single-phase power converters with reduced emi," *IEEE Transactions on Industry Applications*, vol. 53, no. 2, pp. 1300–1307, March 2017.

[9] M. Hartmann, H. Ertl, and J. W. Kolar, "Emi filter design for a 1 mhz, 10 kw three-phase/level pwm rectifier," *IEEE Trans. on Power Electr.*, vol. 26, no. 4, pp. 1192–1204, April 2011.

[10] W. Wu, Y. Sun, Z. Lin, Y. He, M. Huang, F. Blaabjerg, and H. S. h. Chung, "A modified LLCL filter with the reduced conducted EMI noise," *IEEE Transactions on Power Electronics*, vol. 29, no. 7, pp. 3393–3402, July 2014.

[11] S.-J. Kim and S.-K. Sul, "A novel filter design for suppression of high voltage gradient in voltage-fed PWM inverter," in *Proceedings of APEC 97 - Applied Power Electronics Conference*, vol. 1, Feb 1997, pp. 122–127 vol.1.

[12] B. A. Acharya. and V. John, "Common mode dc bus filter for active front-end converter," in *2010 Joint International Conference on Power Electronics, Drives and Energy Systems 2010 Power India*, Dec 2010, pp. 1–6.

[13] D. Barater, G. Buticchi, E. Lorenzani, and C. Concari, "Active common-mode filter for ground leakage current reduction in grid-connected PV converters operating with arbitrary power factor," *IEEE Transactions on Ind. Electron.*, vol. 61, no. 8, pp. 3940–3950, Aug 2014.

[14] J. Huang and H. Shi, "A hybrid filter for the suppression of common-mode voltage and differential-mode harmonics in three-phase inverters with CPPM," *IEEE Transactions on Industrial Electronics*, vol. 62, no. 7, pp. 3991–4000, July 2015.

[15] M. H. Hedayati and V. John, "Emi and ground leakage current reduction in single-phase grid-connected power converter," vol. 10, no. 8, 2017, pp. 938–944.

[16] A. K. Adapa and V. John, "Active phase-converter for operation of three-phase induction motors on single-phase grid," in *IEEE 15th Int. Conf. Power Electron. Drives and Energy Syst. (PEDES), Trivandrum, India*, Dec 2016.

[17] J. A. A. Dias, E. C. dos Santos, C. B. Jacobina, and M. B. R. Correa, "Soft-starting techniques for low cost single-phase to three-phase drive system configuration," in *2008 IEEE Power Electronics Specialists Conference*, June 2008, pp. 3996–4002.

[18] C. S. Lim, E. Levi, M. Jones, N. A. Rahim, and W. P. Hew, "A comparative study of synchronous current control schemes based on fcs-mpc and pi-pwm for a two-motor three-phase drive," *IEEE Transactions on Industrial Electronics*, vol. 61, no. 8, pp. 3867–3878, Aug 2014.

[19] H. Akagi and S. Tamura, "A passive emi filter for eliminating both bearing current and ground leakage current from an inverter-driven motor," *IEEE Transactions on Power Electronics*, vol. 21, no. 5, pp. 1459–1469, Sept 2006.

[20] W. Wu, Y. He, T. Tang, and F. Blaabjerg, "A new design method for the passive damped LCL and LLCL filter-based single-phase grid-tied inverter," *IEEE Transactions on Industrial Electronics*, vol. 60, no. 10, pp. 4339–4350, Oct 2013.